NASA TECHNICAL NOTE

NASA TN D-7471

NASA TN D-7471

A HIGH-PRESSURE CARBON DIOXIDE GASDYNAMIC LASER

by Donald M. Kuehn

Ames Research Center
Moffett Field, Calif. 94035

NATIONAL AERONAUTICS AND SPACE ADMINISTRATION • WASHINGTON, D. C. • NOVEMBER 1973

1. Report No.	2. Government Accession No.	3. Recipient's Catalog No.
NASA TN D-7471		

4. Title and Subtitle	5. Report Date
A HIGH-PRESSURE CARBON DIOXIDE GASDYNAMIC LASER	November 1973
	6. Performing Organization Code

7. Author(s)	8. Performing Organization Report No.
Donald M. Kuehn	A-4993
	10. Work Unit No.
9. Performing Organization Name and Address	503-10-01-01
NASA Ames Research Center Moffett Field, Calif. 94035	11. Contract or Grant No.
	13. Type of Report and Period Covered
12. Sponsoring Agency Name and Address	Technical Note
National Aeronautics and Space Administration Washington, D. C. 20546	14. Sponsoring Agency Code

15. Supplementary Notes

16. Abstract

A carbon dioxide gasdynamic laser was operated over a range of reservoir pressure and temperature, test-gas mixture, and nozzle geometry. A significant result is the dominant influence of nozzle geometry on laser power at high pressure. High reservoir pressure can be effectively utilized to increase laser power if nozzle geometry is chosen to efficiently freeze the test gas. Maximum power density increased from 3.3 W/cm^3 of optical cavity volume for an inefficient nozzle to 83.4 W/cm^3 at 115 atm for a more efficient nozzle. Variation in the composition of the test gas also caused large changes in laser power output. Most notable is the influence of the catalyst (helium or water vapor) that was used to depopulate the lower vibrational state of the carbon dioxide. Water caused an extreme deterioration of laser power at high pressure (100 atm), whereas, at low pressure the laser power for the two catalysts approached similar values. It appears that at high pressure the depopulation of the upper laser level of the carbon dioxide by the water predominates over the lower state depopulation, thus destroying the inversion.

17. Key Words (Suggested by Author(s))	18. Distribution Statement
Gasdynamic laser Carbon dioxide laser High pressure gasdynamic laser	Unclassified – Unlimited

19. Security Classif. (of this report)	20. Security Classif. (of this page)	21. No. of Pages	22. Price*
Unclassified	Unclassified	21	Domestic, $2.75 Foreign, $5.25

* For sale by the National Technical Information Service, Springfield, Virginia 22151

A HIGH–PRESSURE CARBON DIOXIDE GASDYNAMIC LASER

Donald M. Kuehn

Ames Research Center

SUMMARY

Laser power was measured from a carbon dioxide gasdynamic laser for various combinations of test conditions. The optical cavity was nonoptimum; circular mirrors were used with a diameter approximately equal to nozzle height. The experiments were run in a shock tube.

Determination of optimum operating conditions and importance of variables were the prime results of these experiments. An optimum operating temperature was attained for all conditions. The major factors that determine the laser power variation with temperature were the vibrational energy density in the nozzle reservoir, vibrational relaxation in the nozzle, and dissociation of the carbon dioxide. Laser power increased proportionately with reservoir pressure until relaxation of the test gas became significant. In some cases, relaxation caused laser power to go to zero. Geometry of the expansion nozzle was of vital importance to high-pressure operation through its influence on vibrational relaxation. Laser power for one of the nozzles tested peaked out at low pressure and low power, and went to zero at 16 atm pressure. In contrast, an improved nozzle design permitted operation at pressures greater than 100 atm with power increasing proportionately.

Variation in the composition of the test gas caused large changes in the laser power output. Relaxation of the test gas was reduced by using lower concentrations of carbon dioxide. Helium and water vapor as catalysts for depopulating the lower vibrational state of the carbon dioxide resulted in considerably different laser performance. The temperature range over which the gas with water would operate was relatively narrow. In addition, an extreme deterioration of power occurred with the water vapor catalyst at high pressure, whereas at low pressure the two catalysts, in optimum concentrations, were equally effective. The deterioration of power with water was attributed to the predominance of upper state depopulation over the lower state depopulation.

INTRODUCTION

Optimization of test conditions has been shown to be vital to the operation of a carbon dioxide gasdynamic laser (GDL)(e.g., refs. 1-4). This report discusses research on optimization of laser power where the variables were reservoir temperature and pressure, nozzle geometry, test gas composition, and cavity optics. A portion of this work was published in reference 5. It is important to point out that optimization is necessarily for specific sets of conditions and hence precludes generalizations. The purpose of this investigation, therefore, was to obtain experimental data that would define trends rather than to present specific optimization results, with emphasis on the high-pressure test regime where no experiments were available – specifically, at pressures up to 120 atm. Such information should be useful in directing attention to test regimes where substantial gains in laser power output might be attained. In particular, it is expected that these data should be

important to future high-power GDL's that will operate at pressures in the 100-atm range to boost maximum power.

FACILITY AND INSTRUMENTATION

Shock Tube and GDL

A conventional shock tube with a cold helium driver was used in these experiments. Replaceable nozzle blocks fit the inside diameter of the tube (fig. 1(a)). The end portion of the shock tube was the nozzle reservoir. A thin copper diaphragm (0.05 to 0.20 mm) was affixed to the upstream

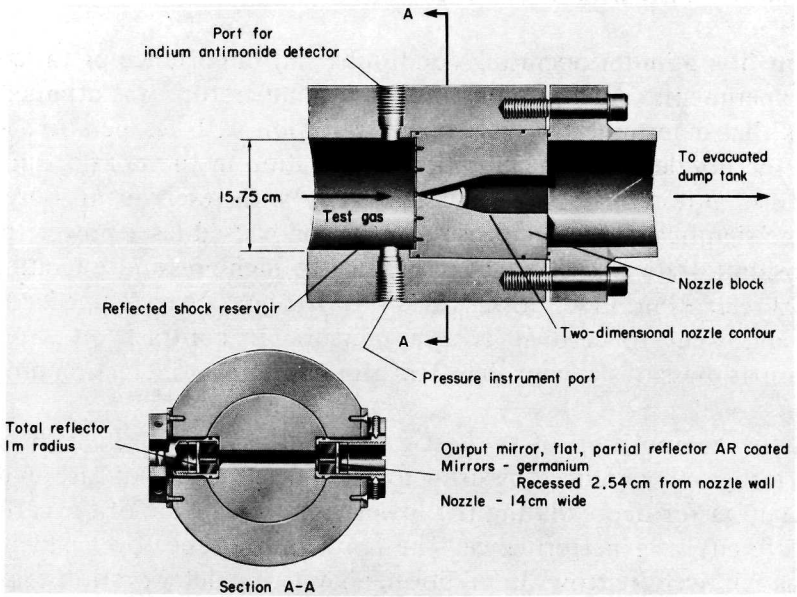

(a) GDL assembly

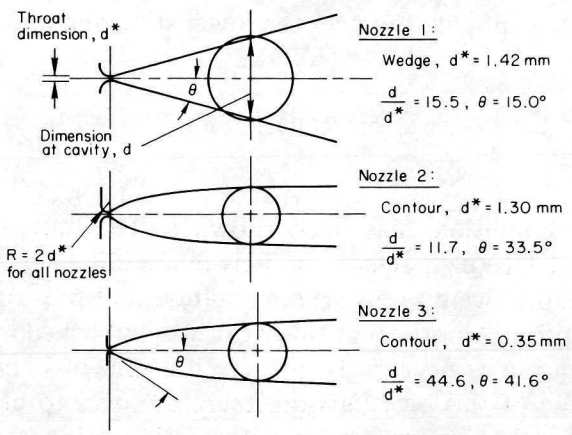

(b) Nozzle contours

Figure 1.– Gasdynamic laser.

face of the nozzle block in the prerun condition to separate the test gas in the shock tube from the evacuated dump tank adjoining the nozzle exit. The diaphragm broke as the incident shock wave was reflected from the nozzle face, and the compressed and heated test gas flowed through the expansion nozzle and into the optical cavity.

Three two-dimensional nozzle contours were designed for these experiments (fig. 1(b)). The function of the nozzle in the GDL is to expand the test gas at a rate that will freeze the vibrational levels of the nitrogen and carbon dioxide at conditions as near as possible to reservoir conditions. The lower vibrational level of the carbon dioxide is generally in equilibrium, so a population inversion in the carbon dioxide is attained. Nozzle design procedures are pursued that will expand the test gas as rapidly as possible. Shaping of the subsonic portion of the nozzle for maximum rate of expansion has been discussed in the literature (e.g., refs. 6 and 7). Specific characteristics that are desirable in the shaping of the supersonic portion of the nozzle can be deduced from some of the early reports that discuss relaxation time as a function of pressure and temperature, and from some of the early discussions of vibrational relaxation in nozzles (e.g., refs. 8-10). More thorough discussions of vibrational relaxation are given in subsequent publications such as reference 11, which describes relaxation of laser gas mixtures.

Maximum freeze efficiency for a nozzle (i.e., the relative effectiveness with which the nozzle produces conditions that promote nonequilibrium) can be attained by using a small throat dimension, maximum rate of expansion equal to one-half the Prandtl-Meyer expansion located at the throat, and a large expansion ratio (i.e., the ratio of area at the optical cavity to that at the nozzle throat). The large expansion ratio gives low pressure and temperature in the nozzle, which in turn results in longer relaxation times. The nozzles shown in figure 1(b) were designed for different freeze efficiencies by varying the throat size, rate of expansion, and expansion ratio (nozzle 1 is the least efficient, while nozzle 3 is the most efficient). The sharp-throat, contoured nozzles represent the minimum length nozzle (expressed in multiples of throat height) with maximum rate of expansion that can be designed for shock-free flow for a chosen value of expansion area ratio.

The optical cavity consisted of two circular mirrors oriented transversely to the nozzle flow; one was a total reflector with a 1-m curvature and the other a flat, germanium mirror coated for partial reflectance. Several values of reflectivity were used. An optical cavity consisting of the 1-m total reflector and a partial reflector with 86.2-percent reflectivity was used in most of the experiments; this will subsequently be referred to as the standard optical cavity. The experiments reported in reference 1 showed that a rapid degradation of mirror reflective surface occurred in only a few runs when surfaces were exposed directly to the main nozzle flow. In the present investigation, therefore, each mirror was recessed 25.4 mm from the nozzle wall, and cylindrical apertures were used with a diameter approximately equal to the nozzle height (apertures were 25.4 mm long, with a diameter of 22.2 mm for nozzle 1 and 15.8 mm for nozzles 2 and 3). This small diameter-to-depth recessed cavity eliminated mirror damage. Reflectivity of the optics, measured with a Coherent Radiation Model 40 laser and a Model 201 power meter, remained constant for the entire series of runs.

It was expected that the aerodynamic flow in the laser cavity would not be disturbed significantly by such a small diameter-to-depth recess. It is not known, however, what effect the mirror recess had on laser power. As the run proceeds, test gas can be trapped in the recess. Initially, this gas will be vibrationally excited, and in sufficient time it will become absorbing. Since time is required for the recess to fill, the effects of these trapped gases will probably be small at the beginning of a laser pulse and become larger near the end. Data to be discussed later show that the

laser power measured near the end of the test time is consistent with that measured early, so the effects of trapped gases seem to be negligible over the test time range used in these experiments.

Instrumentation

The usual instrumentation associated with shock tube research was used for evaluating shock tube performance parameters, such as shock speed and a time history of reservoir pressure; therefore, it will not be described. A significant addition, however, was the indium antimonide, liquid nitrogen-cooled infrared detector, which measured radiation of the carbon dioxide in the reservoir through a sapphire port located 1 in. ahead of the nozzle face. Usable test time was determined by this measurement; the results are discussed later.

The instrumentation to evaluate GDL performance was set up specifically for these experiments. Instantaneous laser power was determined from two measurements – a measure of the total energy of the laser pulse, and a measure of the pulse shape (power vs. time). The primary laser beam was split with a germanium beam splitter. The input face was coated for about 3-percent reflectivity; the back face was AR coated for less than 2-percent reflectivity. A wedged beam splitter was used (ref. 12) and was oriented at an incidence angle of 45°.

The time variation of laser power was measured with a liquid nitrogen-cooled Au-Ge detector. The portion of the laser beam reflected from the splitter was directed to the detector through a 10.6 μm wideband filter with ~3 μm bandpass. Since the sensing element of the detector was only about 1 mm^2, a germanium lens was used to reduce the beam size so that the small-element detector sampled a more representative portion of the beam. In spite of the improvement in sampling afforded by the lens, it became apparent during calibrations of the detector that a direct quantitative measurement of laser power would not be dependable, primarily because the ratio of element size to beam size was not known with sufficient accuracy. However, a method was devised for obtaining a quantitative measurement of power when the detector measurement was used in conjunction with the energy measurement. This method is described in the evaluation of laser power given later.

The energy of the laser beam transmitted by the beam splitter was measured with a calorimeter. The actual pulse energy was obtained by correcting the measured value for reflectivity and absorptivity of the splitter. A sketch of the calorimeter and calibration data is shown in figure 2. The diameter of the copper slug was adequate to measure the laser beam energy by direct impingement in most cases; however, where the beam was slightly larger than the slug or where small misalignment occurred, a highly polished aluminum entrance cone permitted a low-loss reflection of that portion of the beam that did not impinge directly on the slug. A high-absorption black coating was used on the slug to maximize absorptivity. The temperature rise of the slug was measured with a chromel-constantan thermocouple. The mass of the slug was large enough so that the maximum temperature rise was about 10° K (and generally was less than 5° K); thus, the heat loss was small while the temperature of the slug approached equilibrium.

The calorimeter was calibrated using a Coherent Radiation Model 40 laser and Model 201 power meter, and a fast mechanical shutter to vary pulse time. Pulse time was determined from oscilloscope traces of the pulse shape measured with the Au-Ge detector. Various values of laser power and pulse time were used to obtain a range of input energy from less than 1 J to nearly

100 J. The measured energy during calibration (temperature rise of slug X specific heat X weight) was always less than the input energy, but within 10 percent. Errors in the measured values could arise from less than 100-percent absorption plus heat loss; errors in the input energy could be associated with the measurements of the power of the calibration laser and the pulse time.

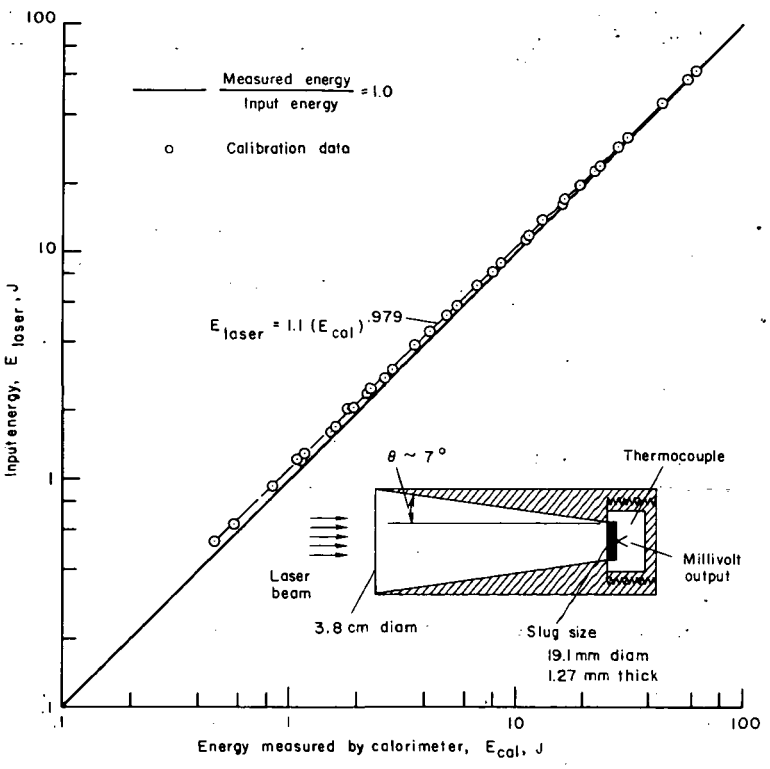

Figure 2.– Description and calibration of calorimeter.

Alignment

Alignment of laser mirrors and instrumentation was important to good data repeatability. An alignment procedure was followed prior to each run. The detailed procedure will not be described; instead, general comments pertaining to the main features of the procedure will be made. Helium-neon lasers on each side of the GDL were the aligning tools. With the aid of small apertures in place of the GDL mirrors, the alignment lasers were adjusted until the beams defined the centerline of the GDL cavity. The beam splitter, calorimeter, and germanium detector could then each be aligned by inserting them into the helium-neon laser beam and fixing their positions on optical bars. The instrumentation was temporarily removed from the optical bars and the GDL mirrors were installed and aligned by reflecting the helium-neon laser beam back on itself. Replacement of the instrumentation on the optical bars completed the alignment.

RESERVOIR CONDITIONS AND LASER POWER EVALUATION

Reservoir conditions and laser power varied with time. It was necessary, therefore, to relate instantaneous reservoir conditions of pressure and temperature with instantaneous laser power. In addition, it was necessary to know the test time for which useful data could be obtained, as determined by the time before the cold helium driver gas begin to mix with and quench the hot test gas.

Test Gas Composition and Purity

All gases used were bottled mixtures with specified concentrations of prepurified grade (or equivalent) components. The shock tube was outgassed by pumping to less than 4 μm many days

before a series of tests and to less than 8 μm pressure for several hours before individual runs. The premixed test gas was loaded in to the tube at load pressures of about 13 to 75 cm of mercury (load pressure for the majority of the runs was greater than 25 cm of mercury). At the minimum loading pressure of the test gas, and the maximum preload pressure, maximum contamination by whatever gases was left in the tube prior to loading was approximately 0.006 percent.

Reservoir Conditions

Time variation of reservoir pressure was measured. An oscilloscope trace of the time variation of pressure is shown at the top of figure 3. Readout was also obtained on a Visicorder for better accuracy. The two sets of traces represent distributions that are typical of low and high shock speeds; the major difference is associated with radiation and will be discussed in the appropriate section. The pressure corresponding to the reflected shock condition is indicated by the inflection in the pressure trace that occurs at a time of about 0.5 to 1.0 msec. This experimental value of pressure agreed with reflected-shock theory, indicating that the theory adequately described the compression associated with the reflected shock wave. A second compression occurred after the reflected pressure rise. Measured reservoir pressure at any time during a run was obtained from these pressure traces.

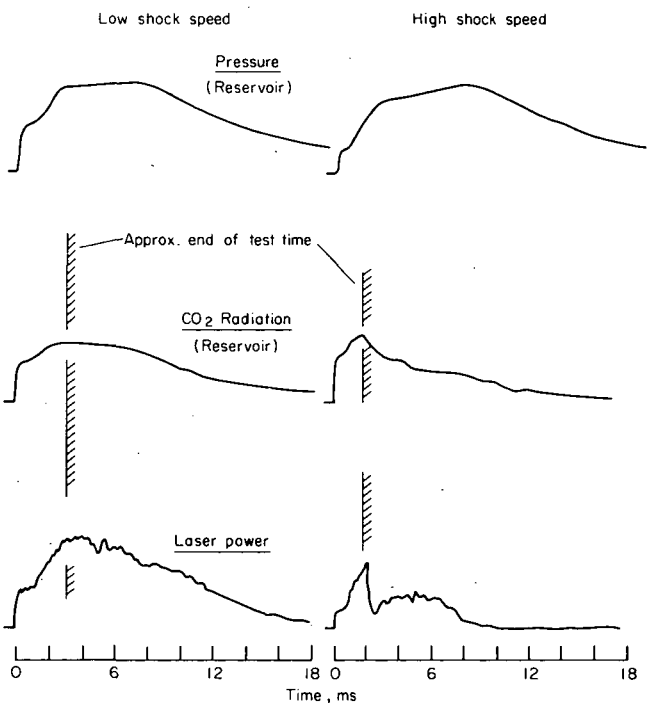

Figure 3.– Measurements of pressure and carbon dioxide radiation in the laser nozzle reservoir, and laser power.

Time variation of reservoir temperature was calculated. The reflected-shock temperature was determined from reflected-shock theory. These values are expected to be reliable since the theory described the pressure rise associated with this compression. Calculated temperature rise during the second compression was based on an isentropic compression.

Evaluation of useful test time was very important to the data analysis. Test time in a shock tube is often a matter of definition, but it is generally accepted that a useful test period occurs at the reflected shock conditions and the time beyond the reflected condition does not represent test time at known conditions with an uncontaminated gas. By contrast, the present evaluation indicates a useful test period that can be longer than the time associated with reflected conditions (see fig. 4), and possibly it could also be shorter at high shock speeds. There might even be no test time at all.

A measurement was made of carbon dioxide radiation in the reservoir with the indium antimonide (In Sb) detector, with a 2 μm filter, that indicates the arrival of the cold helium driver gas. Oscilloscope traces of the In-Sb output and the laser power measured with the Au-Ge detector are

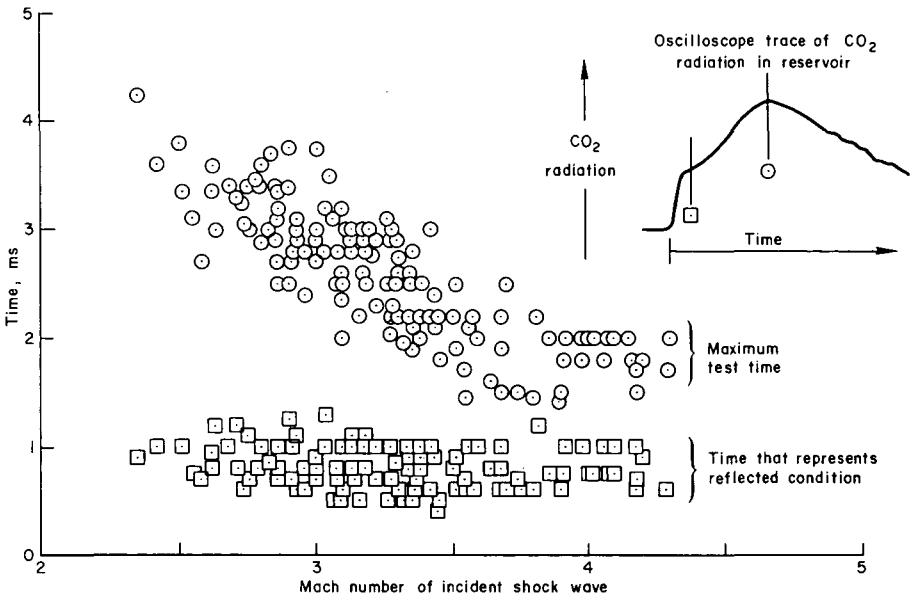

Figure 4.– Test time deduced from the measurement of CO_2 radiation in the reservoir.

shown in figure 3 along with the corresponding pressure traces. Generally, increased pressure and temperature cause an increase in carbon dioxide radiation. The peak radiation that occurs while the pressure is increasing must, therefore, mark the onset of a temperature drop caused by quenching of the test gas by cold driver gas. This quenching occurs earlier in time and more abruptly at higher shock speeds (this point is discussed further in ref. 13).

Lasing continues a considerable time after the beginning of quenching but at conditions that are not known. Typically the laser intensity responds to the pressure-temperature variation with negligible lag; the start time of the nozzle and the flow time between reservoir and cavity are on the order of 0.01 to 0.10 msec, which is not significant in the time scale of the present test times. It is concluded, therefore, that usable test time extends to the peak of the In-Sb measurement, and the instantaneous reservoir conditions that correspond to instantaneous laser power are on the same time scale. Evidence that the test time is indeed useful to this limit and that the corresponding pressure-temperature calculations are reasonably accurate is exhibited by the fact that laser power data from reflected conditions are consistent with data from conditions that correspond to the peak In-Sb output. For example, in figure 8, to be discussed later, the data for nozzle 3 at 25, 40, 50, and 60 atm are at reflected conditions; the data at the other four pressures are at conditions that correspond to the peak for the In-Sb detector.

Evaluation of Laser Power

As discussed earlier, instantaneous laser power was determined from two measurements: total pulse energy measured with the calorimeter, and pulse shape measured with a germanium detector (power vs. time, where scale of the power was not initially known). Since the detector element was

smaller than the beam (see detectors a and b in fig. 5(a)), this measurement gave the time variation of power at some arbitrary location in the beam. Variation of local power over the beam diameter was not known; thus, the distributions shown are schematic. Numerous tests showed that the time variation of power was functionally the same for detectors that sampled different and arbitrary portions of the beam simultaneously during a given test (as shown by the distributions of power, $P_a(t)$ and $P_b(t)$ in fig. 5(b) for detectors a and b). This implies that the time variation of the measured power (detector a for example) was functionally the same as the instantaneous, spatially averaged power ($\overline{P}(t)$) that would be measured with the hypothetical detector c sampling the entire beam, and that the radial distribution of power was functionally the same for all values of time. The time and spatially averaged power $\overline{\overline{P}}$ (still in arbitrary units) can be determined from an integration of $\overline{P}(t)$:

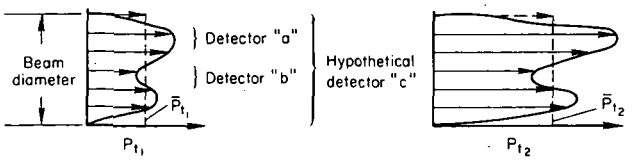

(a) Radial distribution of power

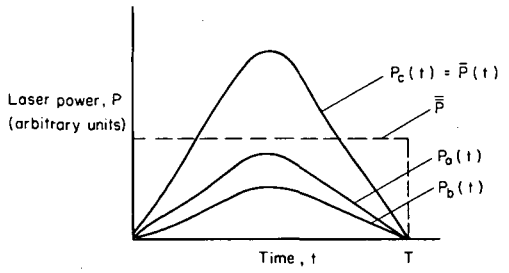

P_t – Local power at time, t

$\overline{P}$ – Spatially averaged power

$\overline{\overline{P}}$ – Time and spatially averaged power

$P_{a,b,c}(t)$ – Power measured by detectors a, b, or c as a function of time

(b) Time variation of power

Figure 5.– Evaluation of laser power.

$$\overline{\overline{P}} = \frac{\int_0^T \overline{P}(t)dt}{T}$$

where T is the laser pulse duration. The instantaneous spatially averaged power (now in watts) at time t is therefore

$$\overline{P}(t) = \overline{\overline{P}} \times \frac{\overline{P}(t)}{\overline{\overline{P}}}$$

$$= \frac{E}{T} \times T\left[\frac{\overline{P}(t)}{\int_0^T \overline{P}(t)\,dt}\right]$$

where the total energy E and the total pulse time T are measured and $\overline{P}(t)/\int_0^T \overline{P}(t)dt$ the term in brackets represents the ratio of ordinate to area under the pulse shape curve (fig. 5(b)). For shapes that are functionally the same (e.g., as from detector a, b, or c), but differ by an area ratio constant, we can write

$$\overline{P}(t) = K_a\overline{P}_a(t) = K_b\overline{P}_b(t)$$

$$\frac{\overline{P}(t)}{\int_0^T \overline{P}(t)dt} = \frac{\overline{P}_c(t)}{\int_0^T \overline{P}_c(t)\,dt} = \frac{\overline{P}_a(t)}{\int_0^T \overline{P}_a(t)dt} = \cdots$$

The measured time variation of power obtained with a small element detector therefore can be used in this evaluation.

RESULTS

Optimization will be discussed in terms of the five test variables: reservoir temperature and pressure, nozzle geometry, test gas, and cavity optics. For all experiments, the diameter of the mirrors in the optical cavity was approximately equal to the nozzle height. Obviously, this small cavity was not designed to extract maximum laser power; thus, any discussion of overall laser efficiency would have no meaning. Since cavity design probably has an influence on optimization, generalization of results is not possible. It is likely, however, that the results of these experiments with a small cavity can define trends, and thus direct attention to test regimes where substantial gains in laser power might be attained, and conversely, point out test regimes where adverse influences might exist. These results will be presented in this light.

Reservoir Temperature

The basic data in this investigation are the variation of laser power with reservoir temperature for various combinations of the other test variables. Examples are shown in figure 6. Typically, laser

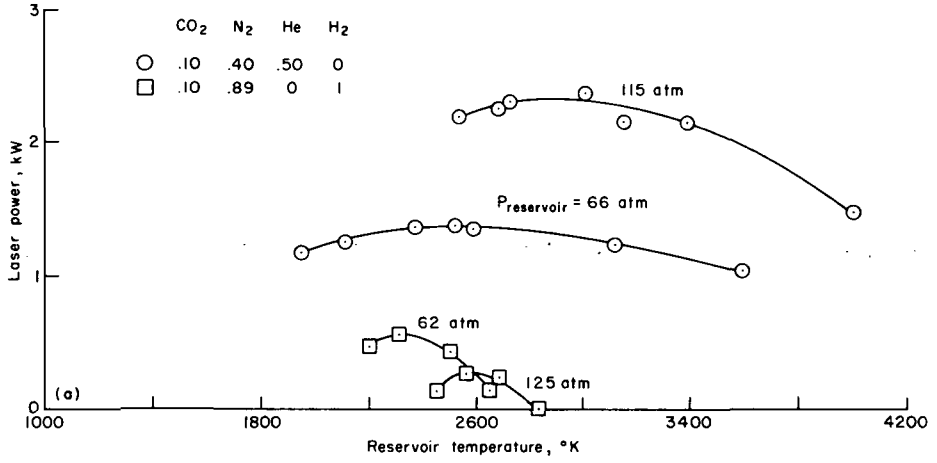

(a) Nozzle 3

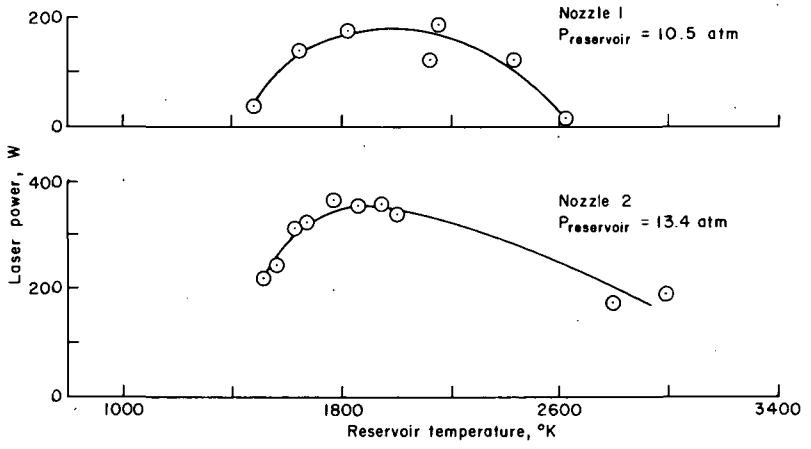

(b) Nozzles 1 and 2; 10 percent CO_2 – 40 percent N_2 – 50 percent He

Figure 6.– Laser power variation with temperature; standard optical cavity.

power increases from zero at some low temperature to a maximum, and then goes to zero again at some higher temperature. Since only the maximum power was of interest, the temperature range was chosen to adequately define the power at optimum temperature rather than establish the temperature range over which lasing would occur. An optimum temperature occurred for all conditions investigated. The value of the optimum temperature is shown in figure 7 for various conditions

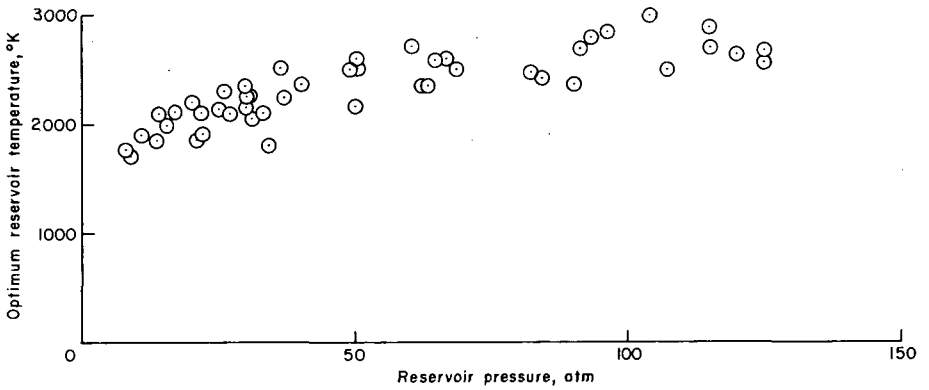

Figure 7.– Optimum reservoir temperature; all nozzles, all test gases.

of nozzle geometry, test gas, and reservoir pressure. Optimum temperature appears to increase with pressure, possibly because there is less dissociation of the carbon dioxide at higher pressures. No systematic variation with nozzle shape or test gas was apparent. These data do scatter considerably, however. Examination of the data in figure 6 indicates that arbitrary curve fitting can cause a variation in optimum temperature of several hundred degrees. This uncertainty could be responsible for the absence of any obvious variation with nozzle shape or test gas. However, the value of maximum power should be more reliable than optimum temperature.

The variation of laser power with temperature is caused by several competing processes. Laser power increases with temperature because the molecular vibrational energy of the test gas in the nozzle reservoir increases. This causes more energy to be available for lasing in the optical cavity, if the vibrational energy freezes out in the initial portion of the nozzle expansion. There are, however, two major factors that tend to reduce energy density in the optical cavity and cause laser power to maximize. First, vibrational energy modes tend to equilibrate in the expansion nozzle as reservoir temperature is increased. A second factor that becomes increasingly significant as temperature is increased is carbon dioxide dissociation in the nozzle reservoir. Together, these factors completely destroy the inversion at sufficiently high temperatures and cause the vibrational energy density in the optical cavity, and the laser power, to go to zero.

The GDL will operate over a very wide temperature range (~1000° K to ~4000° K), but the importance of operating near optimum temperature is obvious. The operating range for a specific laser is significantly affected by nozzle geometry, reservoir pressure, and test gas. The most pronounced influence is shown in figure 6(a) for two different test gases; the laser using helium in the test gas will operate over a temperature range that is many times that for the laser with hydrogen in the test gas. Obviously it is more important to operate close to optimum when hydrogen is used than when helium is used; in fact, at high pressure an error of a few hundred degrees in reservoir temperature could cause the laser that uses hydrogen to not operate at all.

Reservoir Pressure and Nozzle Geometry

Measured laser power is shown in figure 8 for three expansion nozzles and a wide range of reservoir pressure. The value of power was determined at optimum temperature. These data show

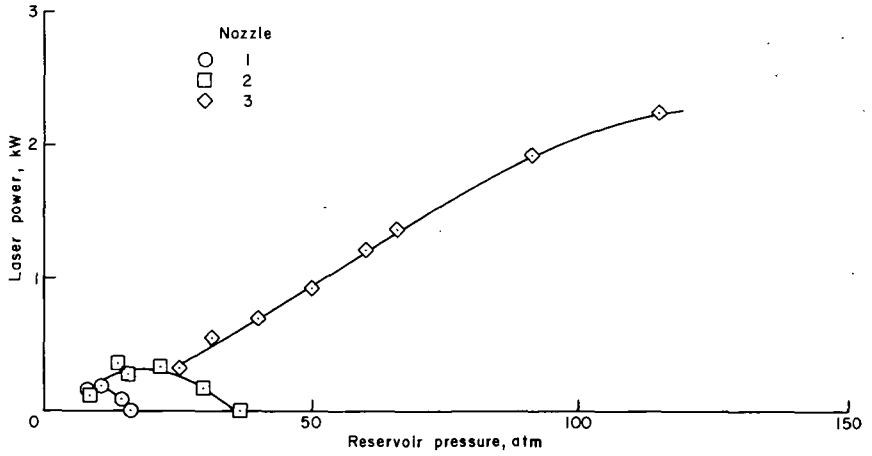

Figure 8.– Laser power variation with reservoir pressure at optimum temperature; standard optical cavity, 10 percent CO_2 – 40 percent N_2 – 50 percent He.

that an optimum pressure (i.e., pressure for maximum power) exists that is associated with nozzle contour; the more rapid expansion permits laser operation at higher pressure, resulting in higher laser power.

The variation of laser power with reservoir pressure is caused primarily by changes in the density of vibrationally excited molecules, and variations in their state of vibrational equilibration. This is shown clearly in the work of Christiansen and Tsongas (ref. 14). Laser power increases proportionately with pressure because the energy density of the test gas is proportional to molecular density. A limitation on power is caused by vibrational relaxation in the expansion nozzle.

Carbon dioxide dissociation is generally present, but is probably not important to the general shape of the power-pressure curves. For example, dissociation is about constant over the pressure range for nozzle 3 because the small increase in dissociation caused by temperature increase is countered by less dissociation as pressure is increased. Further, the amount of dissociation in nozzles 1 and 2 is not enough to cause power to go to zero. It is not likely, then, that dissociation was significant to the trends shown in figure 8; instead, relaxation is probably the primary factor.

The importance of nozzle freeze efficiency in delaying relaxation is clearly demonstrated by these data. Operation of the slow-expansion, low area ratio nozzle is limited to a very narrow pressure range with optimum at 10 atm; maximum power is very low. By contrast, the rapid-expansion, high area ratio nozzle can operate over a very wide pressure range (optimum greater than 120 atm) and thus can achieve high power at high pressure.

Size constraint and mass flow are important features in GDL design. It is interesting, then, to further consider the relative performance of the two lasers with optical cavities of the same size. Comparison of the data in figure 8 for nozzles 2 and 3 leaves no doubt that the small throat, large expansion nozzle offers considerably more operational flexibility. Further, a consideration of mass flow is important to size of equipment. It is apparent that at constant power the mass flow is much lower, or for constant mass flow the power is much higher in the GDL with small throat and large expansion. The mass flow for nozzle 2 at optimum reservoir pressure was approximately equal to that for nozzle 3 at a reservoir pressure of 90 atm. Thus, for equal mass flows and equal sized optical cavities the power of the laser that used the larger expansion area ratio was about 5-1/2 times the power for the other nozzle. Obviously, an efficient nozzle is important to both the low-pressure and the high-pressure GDL, and the use of small throat size and large expansion ratio to attain this efficiency is consistent with sizing constraints.

To compare lasers that have different sized optical cavities, it is useful to normalize laser power with cavity volume. For the data shown in figure 8, these numbers correspond to the maximum power attained for the particular nozzle, and are 3.3, 11.9, and 83.4 W/cm^3 for nozzles 1, 2, and 3, respectively. These numbers demonstrate the superiority of nozzle 3 even more than does the comparison of values of total power because the volume of the optical cavity for nozzle 1 is twice that of nozzle 3. This number also permits a crude comparison of lasers with vastly different optical cavities. For example, the GDLs of the present investigation can be compared with existing low-pressure, high-power lasers where the optical cavity has been optimized for maximum power, and has a very large volume. Generally the output of these high-power lasers is a few watts per cm^3. It is not expected, however, that the same power density attained with a small, nonoptimum cavity can be duplicated by a laser with an optimized cavity because gain generally decreases along the nozzle axis through the cavity. Distribution of power density should also decrease with the result that average power density for the optimized cavity should be lower. The data in figure 8 do suggest, however, that power density might be increased in existing high-power lasers if a high-efficiency expansion nozzle is utilized and the operating conditions are extended to higher reservoir pressure and temperature.

An indication of the area ratio that might be needed at reservoir pressures even higher than used in this investigation can be obtained from the data for the two nozzles with maximum rate of expansion. The static pressure in the optical cavity of nozzle 2 at optimum reservoir pressure is about 0.1 atm. If it can be assumed that the optimum pressure for nozzle 3 will occur in the range of 120 to 140 atm, the corresponding static pressure in the cavity will also be about 0.1 atm. If this reasoning can be extrapolated to higher reservoir pressures, area ratios of about 70 and 110 might be required for reservoir pressures of 200 and 400 atm, respectively. However, this extrapolation must be restricted to maximum expansion rate nozzles and a 10-percent carbon dioxide, 40-percent nitrogen, 50-percent helium test gas; other test gases in other nozzles relax differently.

Test Gas Mixtures

The test gas components in the present experiments were carbon dioxide, nitrogen, helium, and hydrogen. Water vapor is often used instead of hydrogen in carbon dioxide GDLs; in the present investigation hydrogen combines with oxygen in the reservoir to form water vapor (calculations show that nearly all the hydrogen goes to water). The kinetics of this mixture have been discussed in the literature (e.g., refs. 3 and 14), so further discussion here is not necessary. In

general, test gas mixtures for a carbon dioxide GDL are chosen to provide the best compromise between maximum vibrational energy density at reservoir conditions, proper relaxation times to achieve the required differential freezing of the upper and lower laser levels of the carbon dioxide molecule, and selective depopulation of the lower vibrational level of the carbon dioxide to enhance the population inversion. The goal is to deliver maximum vibrational energy available for lasing to the optical cavity with the required inversion. The variations in gas components to be discussed are the ratio of nitrogen to helium with carbon dioxide concentration fixed, variable carbon dioxide concentration, and hydrogen (water vapor) versus helium as catalysts for lower state depopulation.

Nitrogen to helium ratio variable– Consideration of the purpose of the nitrogen and helium components of the test gas leads to the conclusion that an optimum ratio of nitrogen to helium should exist. This is verified by the data in figure 9 describing the variation of laser power with

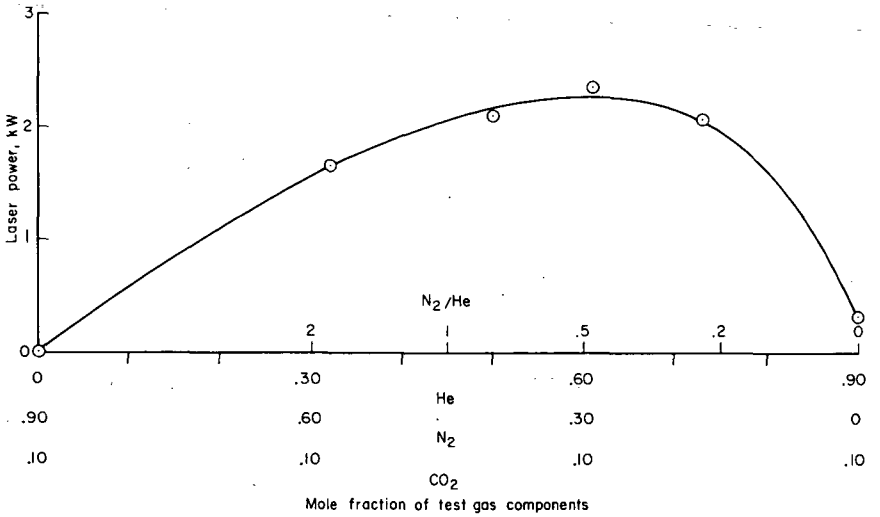

Figure 9.– Laser power for various concentrations of N_2-He in the test gas; reservoir pressure ~100 atm, nozzle 3, standard optical cavity.

nitrogen and helium for nozzle 3 at a reservoir pressure of 100 atm. Energy density of the test gas is a maximum with zero helium concentration because the vibrational energy available for lasing is contained only in the carbon dioxide and nitrogen; the helium contributes no energy to lasing. At this extreme, however, the laser power was zero. The need for helium as a catalyst for depopulation of the lower laser level is, therefore, obvious. This result is consistent with other experiments (e.g., ref. 2) that show absorption, rather than gain, when the mole fraction of helium approaches zero. At the other extreme (i.e., zero nitrogen), the laser did operate but at very low power. The low power was probably a result of low vibrational energy density of the test gas. An optimum is, therefore, to be expected at a ratio that represents a compromise between the benefits derived from the nitrogen and those from the helium. The optimum ratio of nitrogen to helium for the experimental conditions specified was about 0.5, although a significant variation of this ratio appears to be acceptable (like 0.2 to 1.0) with less than a 15-percent loss of power.

Carbon dioxide concentration– Variation of the carbon dioxide concentration provides a means to control relaxation time of a carbon dioxide-nitrogen mixture (ref. 14). Relaxation time is

increased by increasing the ratio of nitrogen to carbon dioxide. Such control is desirable when relaxation of the test gas occurs too rapidly, as when an inefficient expansion nozzle is used, or when the laser is operated at high reservoir pressure and/or temperature. Of course, it is also possible to control the time constant in the opposite direction – that is, to speed up relaxation; however, the case mentioned first is the common occurrence. Since gain is proportional to carbon dioxide concentration, it appears that the proper concentration will be the largest possible consistent with adequate vibrational freezing to assure the necessary population inversion. A more thorough discussion of the kinetics of a carbon dioxide-nitrogen system with variable carbon dioxide concentration is found in reference 14.

Experimental results that demonstrate the influence of variable concentration of carbon dioxide on laser power output are shown in figure 10 for a range of reservoir pressures. The two

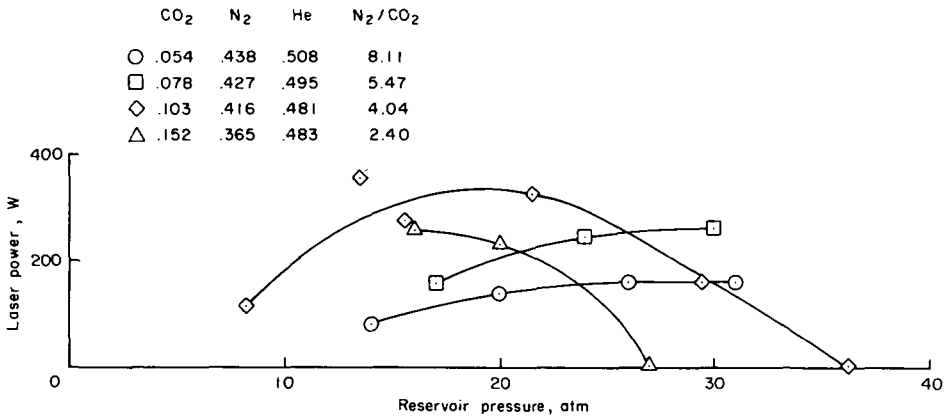

(a) Nozzle 2

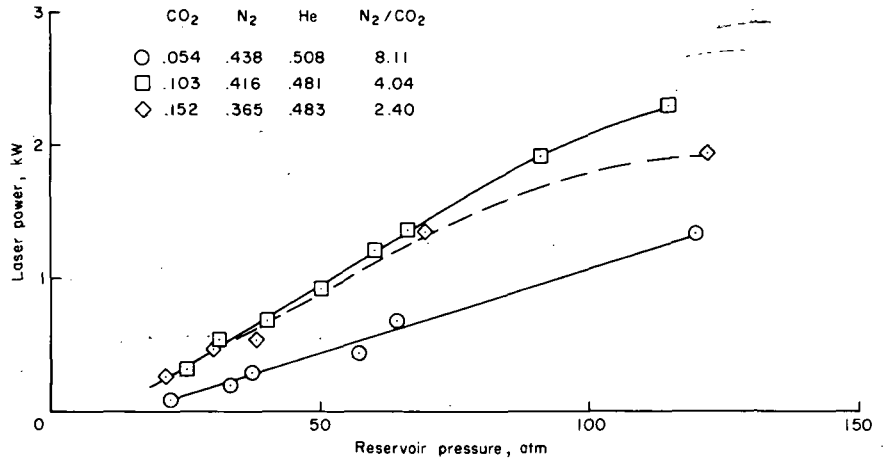

(b) Nozzle 3

Figure 10.– Laser power variation with reservoir pressure for test gases with various concentrations of CO_2; standard optical cavity.

nozzles with maximum rate of expansion were used (nozzles 2 and 3). Previous discussion relating to figure 8 indicated considerable relaxation of the 10-percent carbon dioxide test gas in nozzle 2 (power attained a maximum and went to zero), whereas relaxation in nozzle 3 was, by comparison, not significant. From the discussion in the previous paragraph it might be expected, therefore, that a reduced concentration of carbon dioxide in the laser with nozzle 2 could show significant effects of longer relaxation time, whereas in nozzle 3 such effects should not be large. A longer relaxation time will be evidenced by a delay in the optimum power condition to higher reservoir pressures, with higher power a possible result.

The expected delay of vibrational relaxation due to reduced carbon dioxide concentration did occur, but maximum laser power was attained with the mixture containing 10-percent carbon dioxide. The reservoir pressure for optimum power increased as the carbon dioxide concentration was decreased for the nozzle in which significant relaxation was evident with a 10-percent carbon dioxide gas (fig. 10(a)). The same general trend is apparent for nozzle 3 (fig. 10(b)), although as expected, it is not as obvious. The delay of relaxation caused by decreased concentration of carbon dioxide did not result in higher power for either nozzle, however; instead the gas with 10-percent carbon dioxide was optimum. This result could possibly be due to the fixed size of the optical cavity, and the slower rate of total energy transfer from the nitrogen to the reduced number of carbon dioxide molecules. A longer cavity in the streamwise direction is probably necessary to realize the advantage of reduced carbon dioxide concentration. On the other hand, a question arises whether the longer relaxation time attained with a reduced carbon dioxide concentration is enough to compensate for the increased relaxation associated with a longer cavity. At any rate, with the fixed optical cavity of these experiments, it is not possible to verify that increased power is indeed attainable with reduced carbon dioxide concentration and higher reservoir pressure as suggested in reference 14.

Water vapor and helium as catalysts for lower state depopulation– The two common catalysts for depopulating the lower laser level of the carbon dioxide are helium and water vapor (or hydrogen that will combine with oxygen to form water vapor). Water vapor is the more efficient of the two as evidenced by the mole fraction of each that is required for optimum performance (a few percent for water; about 50 percent for helium). This greater efficiency of water vapor has both advantages and disadvantages. Since all but a few percent of the test gas is carbon dioxide plus nitrogen when hydrogen is used, the energy density for given reservoir conditions is much larger than for the test gas with helium where only 50 percent of the gas has vibrational energy. Laser power could be higher, therefore, with the test gas that contains water vapor if the population inversion is maintained. On the other hand, the greater efficiency of water vapor causes depopulation of the upper laser level (e.g., refs. 11 and 15) as well as the lower level. This will cause a deterioration of the population inversion and a probable decrease of laser power.

The results of experiments to evaluate the influence of helium and water vapor on laser power are shown in figure 11. The most apparent and significant trend shown by these data is the extreme deterioration of laser power at high reservoir pressure caused by water vapor in the test gas. Using the data obtained with a 50-percent helium test gas as a basis for comparison (these data were introduced in fig. 8), it is obvious that an addition of 1-percent hydrogen to this gas has little or no influence at low pressures, but a large power reduction occurs at high pressure. The next two data curves (helium traded for nitrogen; 1-percent hydrogen) show a continuing deterioration of laser power as the helium concentration is reduced to zero. Although the data with reduced helium

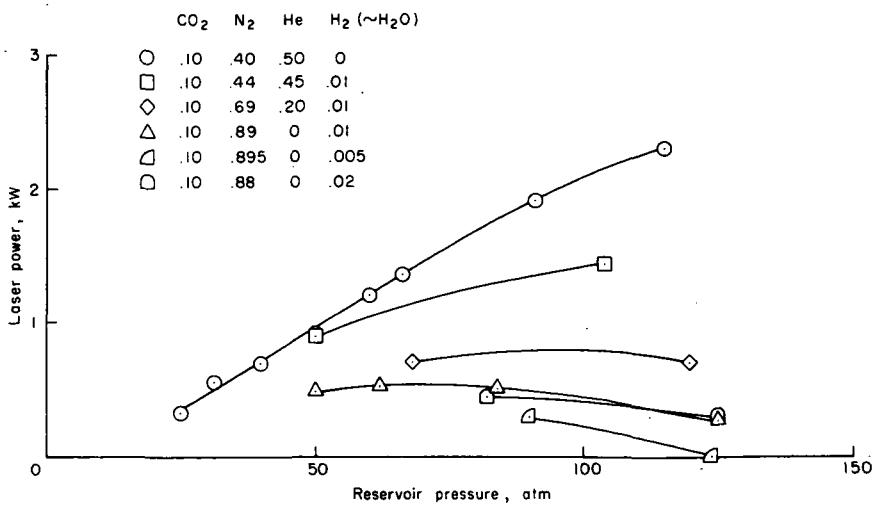

Figure 11.– Laser power variation with pressure for various concentrations of He and/or H_2; nozzle 3, standard optical cavity.

concentration do not extend to low pressures, it appears by extrapolation that the adverse influence of water vapor is small at low pressures and very large at high pressures; in fact, the power has gone nearly to zero at the highest reservoir pressure.

Variation of the water vapor concentration in the test gas has been discussed, usually in terms of gain, in numerous references (e.g., refs. 2-4, 15, 16). It appears generally that concentrations greater than 2 percent can be used, but optimum gain usually occurs with 1- to 2-percent water. An exception appears at very low pressures (e.g., 5 atm) where Tulip and Seguin (ref. 16) showed that gain was relatively constant for concentrations of water vapor up to 8 percent. However, at higher pressure (11 atm in ref. 15) gain decreases rapidly as the water vapor or pressure is increased. The limited data from the present experiments are shown in figures 11 and 12. About all that can be said of these data is that they are consistent with the gain data discussed above in that 1- to 2-percent water vapor is optimum, and the laser power goes to zero at a concentration of water vapor between zero and 1 percent.

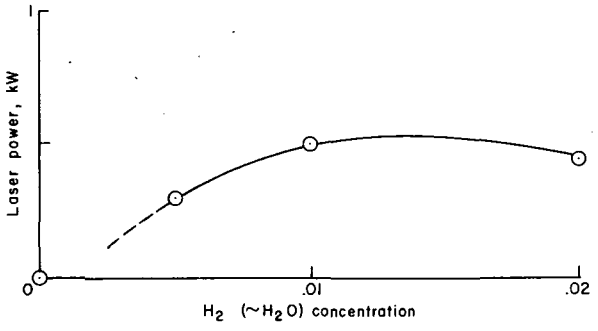

Figure 12.– Influence of H_2 concentration on laser power; pressure ~90 atm, 10 percent CO_2, 90 percent (N_2 + H_2), nozzle 3, standard optical cavity.

The extreme deterioration of laser power at high pressure for the test gases with water vapor is believed to be caused by rapid depopulation of the upper laser level of the carbon dioxide molecule by the water vapor, rather than by relaxation in the nozzle flow. This is deduced from the data in figure 11, which suggest the test gas with hydrogen is nonequilibrium while the laser power approaches zero. Previous discussion, associated with figure 8, indicated that relaxation was negligible for the test gas that contained 50-percent helium (no hydrogen). It seems reasonable to believe, therefore, that vibrational relaxation of the gas with hydrogen is also negligible in view of the work of Christiansen and Tsongas (ref. 14), which shows that

relaxation time of a carbon dioxide-nitrogen mixture is proportional to the ratio of nitrogen to carbon dioxide concentrations. This ratio for the gases with hydrogen is greater than that for the gas with 50-percent helium. Although it is true that the gas without helium expands more slowly than the gas with helium, differences in pressure and temperature are less than a factor of 2. The resulting tendency for faster relaxation of the gas containing hydrogen is compensated to some degree by the longer relaxation times associated with ratios of nitrogen to carbon dioxide that are greater by a factor of 2. If relaxation can be ruled out by such reasoning, it appears that the deterioration of laser power for the gas with hydrogen is probably caused by a deterioration of the population inversion. It is generally accepted that water efficiently depopulates the lower laser level, so a deterioration of the inversion must then be caused by considerable depopulation of the upper vibrational level at high pressure. Thus, even though the energy density of the test gas might be very high, the inversion is destroyed and the laser power goes to zero. A possible conclusion that is consistent with the experiments is that deactivation of the upper laser level by water at high pressure and temperature is simply predominant over the deactivation of the lower state, whereas the opposite is true at lower pressure and temperature.

The conclusion of the previous paragraph is given some support in references 11 and 15. Reference 11 supports the idea that upper state depopulation could predominate at certain conditions. This reference shows that the probability for upper state depopulation by water increases with temperature whereas the probability for lower state depopulation decreases. It is further stated that as a result, water can reduce laser efficiency at high temperatures in contrast to the well-known low temperature enchancement. Calculations in reference 15 support the idea that gain can indeed rapidly go to zero while the test gas is still nonequilibrium. Although not specifically stated, this implies the inversion has gone to zero, possibly by depopulation of the upper vibrational levels.

Since water has such an adverse effect on laser power at high pressure, the obvious suggestion is to vary the gas mixture to reduce the problem. Experiments have not been run to confirm what might happen, but certain arguments can be made. A reduction of the concentration of carbon dioxide is useful to control nitrogen-carbon dioxide relaxation, but it is not likely that this would significantly reduce the upper state depopulation by water. As described in reference 11, water is a very active molecule in all the reactions involving the other gases in the laser gas mixture. If the reaction between water and carbon dioxide is so strong, it seems that a reduction of carbon dioxide could aggravate the situation by reducing even further the number density of carbon dioxide left in the upper excited state, rather than take any carbon dioxide away from the water-carbon dioxide reaction. It might then be suggested that a reduction of the active molecule, water, would reduce its effect on upper state depopulation. This is probably true, but there would also be a reduction of lower state depopulation with no net gain in the inversion. In fact, figure 12 shows that the optimum water concentration is 1 to 2 percent and lower concentrations simply result in lower power. It appears, then, that reduction of water would reduce depopulation of both upper and lower states but would not alter the importance of upper state depopulation relative to lower state depopulation. One might conclude that water in any concentration (and this includes all high-power combustion GDLs where water is a product of combustion) might not be useful as a catalyst for high-pressure GDL operation.

Laser Optics

Reflectivity of the output mirror was varied to obtain some measure of the optimum value for a particular set of conditions. It was not possible in these experiments to optimize the cavity by

altering the streamwise dimension; therefore, reflectivity was varied with fixed diameter optics. For each nozzle geometry, reflectivity was varied at conditions of pressure, temperature and test gas that produced maximum power (shown in fig. 8) with the standard cavity. The experimental data are shown in figure 13. The optimum reflectivity of the output mirror for nozzle 3 was significantly smaller than that for the two nozzles that demonstrated relative inefficiency in establishing a population inversion. Since the power removed from the cavity represents a loss to the cavity, it is reasonable that the most efficient nozzle (which will also have the highest gain) could tolerate the larger losses associated with a lower value of reflectivity. Coincidently, the mirror with 86.2-percent reflectivity initially chosen for the majority of the experiments is very close to the optimum determined for nozzle 3; however, this value of reflectivity is less than the apparent optimum for the other two nozzles.

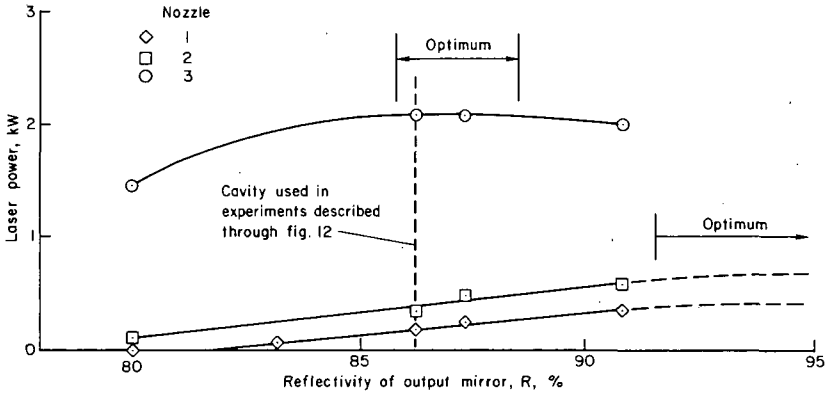

Figure 13.– Laser power variation with reflectivity of the output mirror; test conditions approximately correspond to the optimum shown in figure 8 for nozzles 1 and 2, and 100 atm for nozzle 3.

CONCLUDING REMARKS

Optimum conditions for GDL operation depend on many factors. Since all combinations of variables have not been considered, generalizations cannot be made. Instead, trends that appear generally significant are identified to delineate test regimes where laser power might be increased or difficulties might occur.

Laser power can be increased considerably by operating at high pressure, if the test gas does not relax in the expansion nozzle. Relaxation, however, causes lower, or even zero laser power. The geometry of the expansion nozzle can play a vital role in controlling this relaxation. The present experiments show that a nozzle with a small throat, maximum rate of expansion, and large expansion ratio permits the GDL to operate at a very high pressure with a proportionate increase in power. Such a nozzle is consistent with GDL size constraints; a given optical cavity can produce more power, or the mass flow can be reduced at constant power by utilizing these nozzle design concepts.

Variation of the composition of the test gas offers another means of reducing relaxation. Reduction of the carbon dioxide concentration did delay relaxation as suggested by Christiansen

and Tsongas, but, the expected higher power was not achieved. This contradiction could be caused by the fixed size, nonoptimum cavity used in these experiments.

Whether water vapor or helium was used as a catalyst for lower state depopulation of the carbon dioxide had a significant effect on laser operation. The temperature range over which the laser would operate was relatively small for the test gas that contained water vapor. Further, and most significant, the gas with water vapor caused an extreme deterioration of laser power at high pressures (e.g., 100 atm), whereas at lower pressures the laser power for helium and water vapor catalysts appears to approach similar values. Tentatively, it is concluded that at high pressure and temperature, the depopulation of the upper laser level of the carbon dioxide by water predominates over the lower state depopulation, thus destroying the population inversion. This conclusion raises the question of whether high-power combustion lasers, where water is a product of combustion, can operate effectively at high pressures.

Ames Research Center
National Aeronautics and Space Administration
Moffett Field, Calif. 94035, July 5, 1973

REFERENCES

1. Kuehn, Donald M.; and Monson, Daryl J.: Experiments With a CO_2 Gasdynamic Laser. Appl. Phys. Ltr., vol. 16, no. 1, Jan. 1, 1970, pp. 48-50.

2. Lee, George; Gowen, Forrest E.; and Hagen, Jack. R.: Gain and Power of CO_2 Gas-Dynamic Lasers. AIAA J., vol. 10, no. 1, Jan. 1972, pp. 65-71.

3. Anderson, J. D.; and Harris, E. L.: Modern Advances in the Physics of Gasdynamic Lasers. AIAA paper 72-143, 1972.

4. Meinzer, R. A.: Experimental Gasdynamic Laser Investigation. AIAA paper 71-25, 1971.

5. Kuehn, Donald M.: Importance of Nozzle Geometry to High-Pressure Gasdynamic Lasers. Appl. Phys. Ltr., vol. 21, no. 3, August 1, 1972, pp. 112-114.

6. Greenberg, R. A.; Schneiderman, A. M.; Ahouse, D. R.; and Paramentier, E. M.: Rapid Expansion Nozzles for Gasdynamic Lasers. AIAA paper 72-148, 1972.

7. Wagner, Jerry L.; and Anderson, John D.: An Analytical Investigation of the Effect of Nozzle Throat Radius of Curvature on Gasdynamic Laser Gain. NOLTR 72-51, May 1972.

8. Blackman, Vernon: Vibrational Relaxation in Oxygen and Nitrogen. J. Fluid Mech., vol. 1, May 1956, pp. 61-85.

9. Stollery, J. L.; and Smith, J. E.: A Note on the Variation of Vibrational Temperature Along a Nozzle. J. Fluid Mech., vol. 13, June 1962, pp. 225-236.

10. Erickson, Wayne D.: Vibrational-Nonequilibrium Flow of Nitrogen in Hypersonic Nozzles. NASA TN D-1810, 1963.

11. Taylor, Raymond L.; and Bitterman, Steven: Survey of Vibrational Relaxation Data for Processes Important in the CO_2-N_2 Laser System. Rev. Mod. Phys., vol. 41, no. 1, Jan. 1969, pp. 26-47.

12. Kuehn, Donald M.: Artificial Laser Intensity Oscillations Associated with Beam Splitters. Appl. Opt., vol. 11, no. 6, June 1972, pp. 1431-1433.

13. Monson, D. J.: Measurements of the Duration of Constant Reflected-Shock Temperature in a Reflected-Shock Tunnel. AIAA J., vol. 9, no. 9, Sept. 1971, pp. 1872-1874.

14. Christiansen, Walter H.; and Tsongas, George A.: Gain Kinetics of CO_2 Gasdynamic Laser Mixtures at High Pressure. Phys. Fluids, vol. 14, no. 12, Dec. 1971, pp. 2611-2619.

15. Anderson, John D.: Numerical Experiments Associated with Gasdynamic Lasers. NOLTR 70-198, Sept. 1970.

16. Tulip, J.; and Seguin, H.: Explosion-Pumped Gasdynamic CO_2 Laser. Appl. Phys. Ltr., vol. 19, no. 8, Oct. 15, 1971, pp. 263-265.

NATIONAL AERONAUTICS AND SPACE ADMINISTRATION
WASHINGTON, D.C. 20546

OFFICIAL BUSINESS
PENALTY FOR PRIVATE USE $300

SPECIAL FOURTH-CLASS RATE BOOK

POSTAGE AND FEES PAID
NATIONAL AERONAUTICS AND SPACE ADMINISTRATION
451

U.S.MAIL

POSTMASTER: If Undeliverable (Section 158 Postal Manual) Do Not Return

"The aeronautical and space activities of the United States shall be conducted so as to contribute . . . to the expansion of human knowledge of phenomena in the atmosphere and space. The Administration shall provide for the widest practicable and appropriate dissemination of information concerning its activities and the results thereof."

—NATIONAL AERONAUTICS AND SPACE ACT OF 1958

NASA SCIENTIFIC AND TECHNICAL PUBLICATIONS

TECHNICAL REPORTS: Scientific and technical information considered important, complete, and a lasting contribution to existing knowledge.

TECHNICAL NOTES: Information less broad in scope but nevertheless of importance as a contribution to existing knowledge.

TECHNICAL MEMORANDUMS: Information receiving limited distribution because of preliminary data, security classification, or other reasons. Also includes conference proceedings with either limited or unlimited distribution.

CONTRACTOR REPORTS: Scientific and technical information generated under a NASA contract or grant and considered an important contribution to existing knowledge.

TECHNICAL TRANSLATIONS: Information published in a foreign language considered to merit NASA distribution in English.

SPECIAL PUBLICATIONS: Information derived from or of value to NASA activities. Publications include final reports of major projects, monographs, data compilations, handbooks, sourcebooks, and special bibliographies.

TECHNOLOGY UTILIZATION PUBLICATIONS: Information on technology used by NASA that may be of particular interest in commercial and other non-aerospace applications. Publications include Tech Briefs, Technology Utilization Reports and Technology Surveys.

Details on the availability of these publications may be obtained from:

SCIENTIFIC AND TECHNICAL INFORMATION OFFICE

NATIONAL AERONAUTICS AND SPACE ADMINISTRATION

Washington, D.C. 20546